

Exact and Approximate Formulas for Neutrino Mixing and Oscillations with Non-Standard Interactions

Davide Meloni,^{1,*} Tommy Ohlsson,^{2,†} and He Zhang^{2,‡}

¹*Dipartimento di Fisica, Università di Roma Tre and INFN Sez. di Roma Tre,
via della Vasca Navale 84, 00146 Roma, Italy*

²*Department of Theoretical Physics, School of Engineering Sciences,
Royal Institute of Technology (KTH) – AlbaNova University Center,
Roslagstullsbacken 21, 106 91 Stockholm, Sweden*

Abstract

We present, both exactly and approximately, a complete set of mappings between the vacuum (or fundamental) leptonic mixing parameters and the effective ones in matter with non-standard neutrino interaction (NSI) effects included. Within the three-flavor neutrino framework and a constant matter density profile, a full set of sum rules is established, which enables us to reconstruct the moduli of the effective leptonic mixing matrix elements, in terms of the vacuum mixing parameters in order to reproduce the neutrino oscillation probabilities for future long-baseline experiments. Very compact, but quite accurate, approximate mappings are obtained based on series expansions in the neutrino mass hierarchy parameter $\eta \equiv \Delta m_{21}^2 / \Delta m_{31}^2$, the vacuum leptonic mixing parameter $s_{13} \equiv \sin \theta_{13}$, and the NSI parameters $\varepsilon_{\alpha\beta}$. A detailed numerical analysis about how the NSIs affect the smallest leptonic mixing angle θ_{13} , the deviation of the leptonic mixing angle θ_{23} from its maximal mixing value, and the transition probabilities useful for future experiments are performed using our analytical results.

*Electronic address: meloni@fis.uniroma3.it

†Electronic address: tommy@theophys.kth.se

‡Electronic address: zhanghe@kth.se

I. INTRODUCTION

During the past decade, neutrino oscillation experiments have provided us with very convincing evidence that neutrinos are massive and lepton flavors are mixed [1, 2, 3, 4, 5, 6, 7, 8, 9, 10]. It opens an important window for searching new physics beyond the Standard Model (SM) of particle physics, and has significant cosmological implications. Within the framework of three active neutrinos, neutrino masses are the leading mechanism behind neutrino oscillations [11, 12, 13, 14]. However, in future long-baseline neutrino oscillation experiments, besides the standard matter effects [15, 16], the possibility of testing non-standard neutrino interactions (NSIs) should be opened up.

Note that, NSIs enter neutrino oscillations at production, propagation, and detection processes. In principle, in the case of dimension-6 operators, the corresponding NSI parameters are related to the underlying new physics in the form of $\varepsilon \sim (m_W/m_X)^2$, where m_W is the mass of the W boson and m_X denotes the new physics energy scale. A rough estimate indicates that if new physics appears at the TeV region, the magnitude of NSI parameters should not be larger than a few percent, although the present experimental upper bounds are still very loose. Due to the interference effects, NSIs modify the standard flavor transitions at leading order in ε for some typical processes, especially at a future neutrino factory or other facilities with high-energy beams [17, 18, 19, 20, 21, 22, 23, 24, 25, 26, 27, 28, 29, 30, 31, 32, 33, 34, 35, 36]. In these cases, NSI corrections become particularly relevant, and the experimentally measured values of leptonic mixing angles and CP violating quantities are dramatically different from the vacuum ones. In this sense, the combination of standard neutrino oscillations and NSI effects in the analyses of future neutrino experiments is not only meaningful but also necessary. In addition to NSIs at propagation processes, NSI effects at neutrino sources and detectors play a very important role, since they may induce significant mimicking effects on mixing parameters [37] or bring in distinguishable zero-distance effects for a near detector [38, 39]. Here we will only concentrate on NSIs during the phase of neutrino propagation, and a brief discussion on how to consistently include the source and detector effects will be implemented at the end of Sec. II.

Although much attention has been paid on the issue of NSIs according to different neutrino facilities and projects, the previous analytical investigations are either based on a two-

flavor neutrino framework [40] or an approximation for the three-flavor neutrino oscillation probabilities (indeed producing lengthy formulas). There are still lack of analytical relations, which can show us the NSI effects on the leptonic mixing parameters in a transparent way. Thus, in this paper, we first develop a full set of sum rules, which relate the vacuum leptonic mixing matrix elements and their effective counterparts in matter. By solving these sum rules, it is straightforward to establish the leptonic mixing matrix, unitarity triangles [41], and CP violating effects in matter (see Sec. III). We then present series expansions of mappings in the mass hierarchy parameter $\eta \equiv \Delta m_{21}^2/\Delta m_{31}^2$, the mixing parameter $s_{13} \equiv \sin \theta_{13}$, and the NSI parameters $\varepsilon_{\alpha\beta}$. The NSI corrections to the vacuum mixing parameters can be manifested in a distinct way. We hope that the elegant and compact formulas provided in this paper could be very helpful for the phenomenological studies of future long-baseline neutrino oscillation experiments.

This work is organized as follows. In Sec. II, we present the general formulas and notations, and show how the neutrino oscillation probabilities can be expressed through the language of effective mixing parameters. In Sec. III, we introduce the sum rules between leptonic mixing matrix elements and the effective counterparts in matter, and then derive the mappings exactly. The expressions of effective masses in matter, which are necessary for the calculation of neutrino oscillation probabilities, are shown in detail in Appendix A. Next, in Sec. IV, we derive a full set of series expansions of these mappings. We also compare our mapping results with the corresponding expressions existing in the literature but without NSIs, and find that our results are in agreement with previous analyses in the limit of vanishing NSIs. Section V is devoted to applications of our analytical mappings. Numerical illustrations in order to show the validity and reliability of our approximate results are also presented. Finally, a brief summary is given in Sec. VI.

II. THE LANGUAGE OF EFFECTIVE PARAMETERS

At energy scales $\mu \ll m_W$, the NSIs involving neutrinos can be described by the effective Lagrangian

$$\mathcal{L}_{\text{NSI}} = -\frac{G_F}{\sqrt{2}} \sum_{f,P} \varepsilon_{\alpha\beta}^{fP} (\bar{\nu}_\alpha \gamma^\mu L \nu_\beta) (\bar{f} \gamma_\mu P f) \ , \quad (1)$$

where f is a charged lepton or quark, G_F is the Fermi coupling constant, and $P = \{L, R\}$ is a projection operator. The parameters $\varepsilon_{\alpha\beta}^{fP}$, which are entries of the Hermitian matrix ε^{fP} , give the strengths of the NSIs. The magnitudes of the NSI parameters can be constrained from neutrino deep inelastic scattering experiments and from elastic $\nu-e$ scattering in which the NSIs would contribute to the determination of $\sin^2\theta_W$, i.e., the Weinberg angle. The latest constraints on $\varepsilon_{\alpha\beta}^{fP}$ have been discussed in Ref. [42, 43, 44, 45], and the most stringent bounds are those on $\varepsilon_{\mu\alpha}^{fP}$ for $\alpha = e, \mu, \tau$.

In order to introduce the effective mixing parameters, we start from neutrino oscillations in vacuum. The evolution in time of a neutrino state $|\nu(t)\rangle$ is given by the Schrödinger-like equation

$$i\frac{d}{dt}|\nu(t)\rangle = H|\nu(t)\rangle, \quad (2)$$

where H is the Hamiltonian of the system. For neutrinos traveling in vacuum, the Hamiltonian in the ultra-relativistic limit $E \gg m_i$ reads

$$H = \frac{1}{2E}V\text{diag}(0, \Delta_{21}, \Delta_{31})V^\dagger, \quad (3)$$

where $\Delta_{ij} \equiv m_i^2 - m_j^2$ are the neutrino mass-squared differences and E denotes the neutrino energy. In addition, V is the unitary leptonic mixing matrix [12], which relates the mass eigenstates of the three neutrinos (ν_1, ν_2, ν_3) to their corresponding flavor eigenstates (ν_e, ν_μ, ν_τ)

$$\nu_\alpha = \sum_i V_{\alpha i} \nu_i, \quad (4)$$

for $\alpha = e, \mu, \tau$. For simplicity, the sum of Latin indices run over 1, 2, 3 and the sum of Greek indices run over e, μ, τ throughout this paper, if not otherwise stated. We can define the evolution matrix $S(t, t_0)$ such that

$$|\nu(t)\rangle = S(t, t_0)|\nu(t_0)\rangle, \quad S(t_0, t_0) = 1, \quad (5)$$

and $S(t, t_0)$ satisfies the same Schrödinger-like equation (2), as $|\nu(t)\rangle$. The neutrino oscillation probabilities can be found as $P_{\alpha\beta} = |S_{\beta\alpha}(t, t_0)|^2$. Using Eq. (3), the elements of the evolution matrix are given by

$$S_{\beta\alpha}(t, t_0) = \sum_i V_{\alpha i} V_{\beta i}^* e^{-i\frac{m_i^2 L}{2E}}, \quad (6)$$

where we have identified $L \equiv t - t_0$. Thus, the probability of transition from a neutrino flavor α to a neutrino flavor β is given by

$$P_{\alpha\beta} \equiv |S_{\beta\alpha}(t, t_0)|^2 = \left| \sum_i V_{\alpha i} V_{\beta i}^* e^{-i \frac{m_i^2 L}{2E}} \right|^2. \quad (7)$$

For the setups of future long-baseline neutrino oscillation experiments, the neutrino beams inevitably travel through the Earth's mantle, and the charged-current contributions to the matter-induced effective potential have to be considered properly. Disregarding the neutral-current contributions, the effective Hamiltonian responsible for neutrino propagation in matter is given by

$$\tilde{H}_{\alpha\beta} = H_{\alpha\beta} + a (\delta_{\alpha e} \delta_{\beta e} + \varepsilon_{\alpha\beta}), \quad (8)$$

where the matter parameter $a = \sqrt{2} G_F N_e$ arises from coherent forward scattering. Here N_e denotes the electron number density along the neutrino trajectory in the Earth and the NSI parameters $\varepsilon_{\alpha\beta}$ are defined as

$$\varepsilon_{\alpha\beta} = \sum_{f,P} \varepsilon_{\alpha\beta}^{fP} \frac{N_f}{N_e}, \quad (9)$$

with N_f being the number density of a fermion of type f .

Similar to the vacuum Hamiltonian in Eq. (3), the effective Hamiltonian in matter can also be diagonalized through a unitary transformation

$$\tilde{H} = \frac{1}{2E} \tilde{V} \text{diag} (\tilde{m}_1^2, \tilde{m}_2^2, \tilde{m}_3^2) \tilde{V}^\dagger, \quad (10)$$

where \tilde{m}_i^2 denote the effective mass-squared eigenvalues of neutrinos and \tilde{V} is the unitary mixing matrix in matter. Note that, in writing down Eq. (10), we have already taken into account the Hermitian property of \tilde{H} .

In order to write out explicitly the transition probabilities, we assume a constant matter density profile, which is actually close to reality for most of the proposed long-baseline experiments. Following analogous procedures as shown in Eqs. (4)-(7), one can then obtain the transition probabilities with matter effects included as

$$P_{\alpha\beta} \equiv |S_{\beta\alpha}(t, t_0)|^2 = \left| \sum_i \tilde{V}_{\alpha i} \tilde{V}_{\beta i}^* e^{-i \frac{\tilde{m}_i^2 L}{2E}} \right|^2. \quad (11)$$

Comparing Eq. (7) with Eq. (11), we arrive at the conclusion that there is no difference between the form of the neutrino oscillation probabilities in vacuum and in matter if we replace the vacuum parameters V and m_i^2 by the effective parameters \tilde{V} and \tilde{m}_i^2 . The mappings between vacuum parameters and the effective ones are sufficient in order to study the new physics effects entering future long-baseline neutrino oscillation experiments. The key point turns out to be the diagonalization of the effective Hamiltonian \tilde{H} and figuring out the explicit relations of the effective parameters.

In most of the viable models for NSIs, the source and detector effects are simultaneously taken into account, despite their magnitude. The language of effective mixing parameters can then easily be extended to the case including NSIs at neutrino sources and detectors. Now, the NSI parameters at sources and detectors can be defined as [17, 31, 46]

$$|\nu_\alpha^s\rangle = |\nu_\alpha\rangle + \sum_{\beta=e,\mu,\tau} \varepsilon_{\alpha\beta}^s |\nu_\beta\rangle, \quad (12)$$

$$\langle\nu_\beta^d| = \langle\nu_\beta| + \sum_{\alpha=e,\mu,\tau} \varepsilon_{\alpha\beta}^d \langle\nu_\alpha|, \quad (13)$$

where the superscripts ‘s’ and ‘d’ denote source and detector, respectively. The transition probabilities are then modified as¹

$$\begin{aligned} P_{\alpha\beta} &= \left| \left[(1 + \varepsilon^d)^T \cdot S(t, t_0) \cdot (1 + \varepsilon^s)^T \right]_{\beta\alpha} \right|^2 \\ &= \left| \sum_{\gamma,\delta,i} (1 + \varepsilon^d)_{\gamma\beta} (1 + \varepsilon^s)_{\alpha\delta} \tilde{V}_{\delta i} \tilde{V}_{\gamma i}^* e^{-i\frac{\tilde{m}_i^2 L}{2E}} \right|^2. \end{aligned} \quad (14)$$

Note that Eq. (14) is also suitable to describe neutrino oscillations with a non-unitary mixing matrix, i.e., the minimal unitarity violation model [47]. In the following sections, we will only concentrate on NSI effects during propagation processes and establish parameter mappings both exactly and approximately.

III. SUM RULES AND PARAMETER MAPPINGS

In order to establish analytical relations between the matrix elements of \tilde{V} and those of V , we develop a set of sum rules, which enables us to express the products $\tilde{V}_{\alpha i} \tilde{V}_{\beta i}^*$ by using

¹ Here we have neglected the normalization factors, which are needed in order to normalize the quantum states.

V , m_i^2 and \tilde{m}_i^2 . Such an approach has partially been employed in Refs. [48, 49, 50] in the case of three or four-neutrino mixing. Here we will work out the most general form with both the standard matter effects and the NSI effects included.

The first sum rule is just the unitarity conditions, which hold for both \tilde{V} and V ,

$$\sum_i \tilde{V}_{\alpha i} \tilde{V}_{\beta i}^* = \sum_i V_{\alpha i} V_{\beta i}^* = \delta_{\alpha\beta} . \quad (15)$$

Inserting Eqs. (3) and (10) into Eq. (8), and comparing both sides of this result, it is straightforward to obtain the second sum rule

$$\sum_i \tilde{m}_i^2 \tilde{V}_{\alpha i} \tilde{V}_{\beta i}^* = \sum_i \Delta_{i1} V_{\alpha i} V_{\beta i}^* + \mathcal{A}_{\alpha\beta} , \quad (16)$$

where we have defined $\mathcal{A}_{\alpha\beta} \equiv A (\delta_{\alpha e} \delta_{\beta e} + \varepsilon_{\alpha\beta})$ with $A \equiv 2Ea$ for simplicity. In order to derive a linearly independent sum rule besides the first two, we square both sides of Eq. (16) and obtain the squared relation

$$\sum_i \tilde{m}_i^4 \tilde{V}_{\alpha i} \tilde{V}_{\beta i}^* = \sum_i \Delta_{i1}^2 V_{\alpha i} V_{\beta i}^* + \sum_{\gamma} \mathcal{A}_{\alpha\gamma} \mathcal{A}_{\beta\gamma}^* + \sum_{\gamma, i} \Delta_{i1} (\mathcal{A}_{\alpha\gamma} V_{\gamma i} V_{\beta i}^* + \mathcal{A}_{\beta\gamma}^* V_{\alpha i} V_{\gamma i}^*) . \quad (17)$$

Equations (16)-(17) together with the unitarity condition Eq. (15) construct a full set of linear equations of $\tilde{V}_{\alpha i} \tilde{V}_{\beta i}^*$ (for $i = 1, 2, 3$). By solving this set of equations, one will arrive at the explicit expressions of $\tilde{V}_{\alpha i} \tilde{V}_{\beta i}^*$ straightforwardly.

In order to be concrete, we reexpress those equations in the following form

$$\begin{aligned} \tilde{O} \begin{pmatrix} \tilde{V}_{\alpha 1} \tilde{V}_{\beta 1}^* \\ \tilde{V}_{\alpha 2} \tilde{V}_{\beta 2}^* \\ \tilde{V}_{\alpha 3} \tilde{V}_{\beta 3}^* \end{pmatrix} &= O \begin{pmatrix} V_{\alpha 1} V_{\beta 1}^* \\ V_{\alpha 2} V_{\beta 2}^* \\ V_{\alpha 3} V_{\beta 3}^* \end{pmatrix} + \begin{pmatrix} 0 \\ \mathcal{A}_{\alpha\beta} \\ \sum_{\gamma} \mathcal{A}_{\alpha\gamma} \mathcal{A}_{\beta\gamma}^* \end{pmatrix} \\ &+ Q \sum_{\gamma} \left[\mathcal{A}_{\alpha\gamma} \begin{pmatrix} V_{\gamma 1} V_{\beta 1}^* \\ V_{\gamma 2} V_{\beta 2}^* \\ V_{\gamma 3} V_{\beta 3}^* \end{pmatrix} + \mathcal{A}_{\beta\gamma}^* \begin{pmatrix} V_{\alpha 1} V_{\gamma 1}^* \\ V_{\alpha 2} V_{\gamma 2}^* \\ V_{\alpha 3} V_{\gamma 3}^* \end{pmatrix} \right] , \end{aligned} \quad (18)$$

where the matrices \tilde{O} , O , and Q are defined by

$$\tilde{O} = \begin{pmatrix} 1 & 1 & 1 \\ \tilde{m}_1^2 & \tilde{m}_2^2 & \tilde{m}_3^2 \\ \tilde{m}_1^4 & \tilde{m}_2^4 & \tilde{m}_3^4 \end{pmatrix} , \quad O = \begin{pmatrix} 1 & 1 & 1 \\ 0 & \Delta_{21} & \Delta_{31} \\ 0 & \Delta_{21}^2 & \Delta_{31}^2 \end{pmatrix} , \quad Q = \begin{pmatrix} 0 & 0 & 0 \\ 0 & 0 & 0 \\ 0 & \Delta_{21} & \Delta_{31} \end{pmatrix} . \quad (19)$$

After a lengthy calculation, the solution of Eq. (18) can be presented in a very elegant and compact form

$$\begin{aligned} \tilde{V}_{\alpha i} \tilde{V}_{\beta i}^* = & \frac{1}{\tilde{\Delta}_{im} \tilde{\Delta}_{in}} \left[\sum_j \hat{\Delta}_{jm} \hat{\Delta}_{jn} V_{\alpha j} V_{\beta j}^* - \mathcal{A}_{\alpha\beta} (\tilde{m}_n^2 + \tilde{m}_m^2) \right. \\ & \left. + \sum_{\gamma} \mathcal{A}_{\alpha\gamma} \mathcal{A}_{\beta\gamma}^* + \sum_{\gamma, j} \Delta_{j1} (\mathcal{A}_{\alpha\gamma} V_{\gamma j} V_{\beta j}^* + \mathcal{A}_{\beta\gamma}^* V_{\alpha j} V_{\gamma j}^*) \right], \end{aligned} \quad (20)$$

where $i \neq n \neq m$, $\tilde{\Delta}_{ij} = \tilde{m}_i^2 - \tilde{m}_j^2$, and $\hat{\Delta}_{ij} = m_i^2 - m_1^2 - \tilde{m}_j^2$. Note that the pairs $(m, n) = (2, 3), (3, 1), (1, 2)$ in the right-hand side correspond to $i = 1, 2, 3$ in the left-hand side, respectively. Equation (20) is our main result for the exact analytical mappings.

The full mappings require the explicit form of \tilde{m}_i^2 , which involves the cubic roots of the characteristic polynomial of Eq. (8). We follow the method given in Ref. [51], and the corresponding roots (or eigenvalues) can be found in Appendix A. One may worry about the \tilde{m}_i^2 's appearing in Eq. (20), since it seems that the effective mixing matrix elements rely on the absolute effective neutrino masses. However, recalling the solutions in Eqs. (A4)-(A6), it is easy to observe that only the mass-squared differences enter into the expressions of \tilde{m}_i^2 , and it guarantees the consistency of our calculations. Obviously, $\mathcal{A}_{\alpha\beta} = 0$ leads to $\tilde{V}_{\alpha i} \tilde{V}_{\beta i}^* = V_{\alpha i} V_{\beta i}^*$. In the limit $\varepsilon_{\alpha\beta} \rightarrow 0$, Eq. (20) reduces to the case of standard matter effects, and the main results given in Refs. [48, 49, 52, 53, 54] will be easily reproduced. These exact relations are model independent and do not rely on any specific parametrization, and hence, it will be very helpful to systematically study NSIs in future experiments.

Taking $\alpha = \beta$, the moduli of $\tilde{V}_{\alpha i}$ can be estimated immediately. For the case $\alpha \neq \beta$, the sides of leptonic unitarity triangles, which are defined by the orthogonality relations in Eq. (15) in the complex plane, are obtained. These unitarity triangles have 18 different sides and nine different inner angles, but their areas are all identical to a single rephasing-invariant parameter $\mathcal{J}/2$ defined through [55]

$$\text{Im}(V_{\alpha i} V_{\beta j} V_{\alpha j}^* V_{\beta i}^*) = \mathcal{J} \sum_{\gamma, k} (\epsilon_{\alpha\beta\gamma} \epsilon_{ijk}). \quad (21)$$

One of the major challenges of future long-baseline neutrino oscillation experiments is to measure \mathcal{J} , in order to establish the existence of CP violation in the lepton sector. We can also define the counterpart of \mathcal{J} in matter as $\tilde{\mathcal{J}}$. Its magnitude is related to the moduli of

the effective mixing matrix elements as

$$\begin{aligned} \tilde{\mathcal{J}}^2 = & |\tilde{V}_{\alpha i}|^2 |\tilde{V}_{\beta j}|^2 |\tilde{V}_{\alpha j}|^2 |\tilde{V}_{\beta i}|^2 - \frac{1}{4} \left(1 + |\tilde{V}_{\alpha i}|^2 |\tilde{V}_{\beta j}|^2 + |\tilde{V}_{\alpha j}|^2 |\tilde{V}_{\beta i}|^2 \right. \\ & \left. - |\tilde{V}_{\alpha i}|^2 - |\tilde{V}_{\beta j}|^2 - |\tilde{V}_{\alpha j}|^2 - |\tilde{V}_{\beta i}|^2 \right)^2 . \end{aligned} \quad (22)$$

As an application, we show, in Appendix B, the zeroth-order series expansions of $|\tilde{V}_{e3}|^2$, $|\tilde{V}_{e2}|^2$, and $|\tilde{V}_{\mu 3}|^2$ in small parameters, i.e., η and V_{e3} . In addition, simplified formulas of Eq. (20) and the effective mixing matrix elements for standard matter effects are presented in Appendix B.

Now, the neutrino oscillation probabilities can be directly obtained with the help of Eq. (11) for a realistic experiment. In order to be explicit, we can express the neutrino oscillation probabilities in matter as

$$P_{\alpha\alpha} = 1 - 4 \sum_{i>j} |\tilde{V}_{\alpha i} \tilde{V}_{\alpha j}^*|^2 \sin^2 \left(\frac{\tilde{\Delta}_{ij} L}{4E} \right) , \quad (23)$$

$$P_{\alpha\beta} = -4 \sum_{i>j} \text{Re} \left(\tilde{V}_{\alpha i}^* \tilde{V}_{\beta i} \tilde{V}_{\alpha j} \tilde{V}_{\beta j}^* \right) \sin^2 \left(\frac{\tilde{\Delta}_{ij} L}{4E} \right) - 8\tilde{\mathcal{J}} \prod_{i>j} \sin \left(\frac{\tilde{\Delta}_{ij} L}{4E} \right) , \quad (24)$$

where (α, β) run over (e, μ) , (μ, τ) , and (τ, e) . For anti-neutrino propagation in matter, we can simply recalculate Eqs. (23) and (24) through the replacements $A \rightarrow -A$, $V_{\alpha i} \rightarrow V_{\alpha i}^*$, and $\varepsilon_{\alpha\beta} \rightarrow \varepsilon_{\alpha\beta}^*$. In general, note that $\tilde{V}_{\alpha i}$, $\tilde{\Delta}_{ij}$ and $\tilde{\mathcal{J}}$ for neutrinos are not identical to $\tilde{V}_{\alpha i}$, $\tilde{\Delta}_{ij}$ and $\tilde{\mathcal{J}}$ for anti-neutrinos. At first glance, one may wonder if the information on the phases of $\varepsilon_{\alpha\beta}$ have been lost, since there is only one parameter \mathcal{J} governing the CP-violating effects. We stress that, in neglecting the NSIs at sources and detectors, flavor and mass eigenstates of neutrinos can always be correlated by using a unitary transformation, and hence, we can use one effective rephasing invariant to describe the CP-violating effects in neutrino oscillations. For instance, if we ignore the source and detector effects in Eq. (33) of Ref. [31], the remaining CP-odd terms can be combined together with respect to a common oscillating factor, which is consistent with our compact formulas (23) and (24).

Although our exact analytical results are very elegant, they do not show how new physics affects mixing parameters in a transparent way. From a phenomenological point of view, analytically approximate mappings are very useful, since they can reveal the underlying correlations between effective mixing parameters and NSI effects, and in particular, show which of them are mostly relevant for a given process. In the following section, we will

perform a detailed analysis of approximate mappings based on series expansions in small mixing parameters and NSI corrections. This method is indeed similar to the analysis of series expansion formulas for neutrino oscillation probabilities [56].

IV. SERIES EXPANSIONS OF PARAMETER MAPPINGS

In this section, we proceed to present the series expansion formulas of parameter mappings in η , s_{13} , and the NSI parameters $\varepsilon_{\alpha\beta}$. For convenience, we adopt the standard parametrization and thus the vacuum leptonic mixing matrix V can be parametrized by using three mixing angles and one CP violating phase as

$$\begin{aligned}
V &= O_{23}V_\delta O_{13}V_\delta^\dagger O_{12} \\
&= \begin{pmatrix} c_{12}c_{13} & s_{12}c_{13} & s_{13}e^{-i\delta} \\ -s_{12}c_{23} - c_{12}s_{23}s_{13}e^{i\delta} & c_{12}c_{23} - s_{12}s_{23}s_{13}e^{i\delta} & s_{23}c_{13} \\ s_{12}s_{23} - c_{12}c_{23}s_{13}e^{i\delta} & -c_{12}s_{23} - s_{12}c_{23}s_{13}e^{i\delta} & c_{23}c_{13} \end{pmatrix}, \quad (25)
\end{aligned}$$

where $V_\delta = \text{diag}(1, 1, e^{i\delta})$, and O_{ij} is the orthogonal rotation matrix in the (i, j) -plane with $c_{ij} \equiv \cos \theta_{ij}$ and $s_{ij} \equiv \sin \theta_{ij}$ (for $ij = 12, 13, 23$). A global analysis of current experimental data yields $0.25 < \sin^2 \theta_{12} < 0.37$, $0.36 < \sin^2 \theta_{23} < 0.67$, and $\sin^2 \theta_{13} < 0.056$ at the 3σ confidence level, but the CP-violating phase δ is entirely unrestricted [57]. The best-fit values of neutrino mass-squared differences are $\Delta_{21} = 7.65 \times 10^{-5} \text{ eV}^2$ and $|\Delta_{31}| = 2.4 \times 10^{-3} \text{ eV}^2$, which indicate that the hierarchy parameter we defined in Sec. I is given by $\eta \equiv \Delta_{21}/\Delta_{31} \simeq \pm 0.032$. Present experimental bounds on the NSI parameters $\varepsilon_{\alpha\beta}$ show that $\varepsilon_{\mu\alpha}$ (or $\varepsilon_{\alpha\mu}$) are strongly constrained to $|\varepsilon_{e\mu}| \lesssim 3.8 \times 10^{-4}$ and $-0.05 < \varepsilon_{\mu\mu} < 0.08$ at 90 % confidence level [30]. This is the reason why some of the previous works neglect contributions of $\varepsilon_{\mu\alpha}$ [40]. In the following, we will only focus on $\varepsilon_{e\tau}$, $\varepsilon_{\mu\tau}$, $\varepsilon_{\mu\mu}$, and $\varepsilon_{\tau\tau}$ contributions, respectively.

Using a similar notation, one may also define the effective mixing angles $\tilde{\theta}_{12}$, $\tilde{\theta}_{13}$, $\tilde{\theta}_{23}$, and CP violating phase $\tilde{\delta}$ in matter. Then, we can parameterize \tilde{V} in analogy to Eq. (25). It is straightforward to extract the sines of the mixing angles from Eq. (25) using

$$s_{13} = |V_{e3}|, \quad s_{12} = |V_{e2}|/\sqrt{1 - |V_{e3}|^2}, \quad s_{23} = |V_{\mu 3}|/\sqrt{1 - |V_{e3}|^2}. \quad (26)$$

The effective mixing angles $\tilde{\theta}_{ij}$ are obtainable once the moduli of $\tilde{V}_{\alpha\beta}$ are computed using Eq. (20), and it is not difficult to check that in the limit of vanishing matter effects the

effective mixing angles are equal to the vacuum ones. Analytical relations between $\tilde{\theta}$ and θ could be very useful and they rely on the perturbation theory that we have employed.

For our purposes, we first factor out the rotation matrix O_{23}

$$\begin{aligned}\tilde{H} &= \frac{\Delta_{31}}{2E} O_{23} V_\delta \cdot M \cdot V_\delta^\dagger O_{23}^T \\ &= \frac{\Delta_{31}}{2E} O_{23} V_\delta \cdot \left[\hat{V} \cdot \text{diag}(\lambda_1, \lambda_2, \lambda_3) \cdot \hat{V}^\dagger \right] \cdot V_\delta^\dagger O_{23}^T, \end{aligned} \quad (27)$$

where M is given by

$$M = O_{13} O_{12} \cdot \text{diag}(0, \eta, 1) \cdot O_{12}^T O_{13}^T + \text{diag}(\hat{A}, 0, 0) + V_\delta^\dagger O_{23}^T \cdot \varepsilon \cdot O_{23} V_\delta, \quad (28)$$

and $\hat{A} \equiv A/\Delta_{31}$. In deriving Eq. (27), the following commutative properties are used

$$V_\delta^\dagger O_{12} = O_{12} V_\delta^\dagger, \quad (29)$$

$$V_\delta^\dagger \cdot \text{diag}(\hat{A}, 0, 0) = \text{diag}(\hat{A}, 0, 0) \cdot V_\delta^\dagger. \quad (30)$$

The diagonalization of M is performed by using perturbation theory, i.e., we write $M = M^{(0)} + M^{(1)} + \dots$, where $M^{(1)}$ contains all terms of first order in η , s_{13} , and $\varepsilon_{\alpha\beta}$. One finds

$$M^{(0)} = \text{diag}(\hat{A}, 0, 1) = \text{diag}(\lambda_1^{(0)}, \lambda_2^{(0)}, \lambda_3^{(0)}), \quad (31)$$

and

$$M^{(1)} = \begin{pmatrix} \eta s_{12}^2 + \hat{A} \hat{\varepsilon}_{ee} & \eta s_{12} c_{12} + \hat{A} \hat{\varepsilon}_{e\mu} & s_{13} e^{-i\delta} + \hat{A} \hat{\varepsilon}_{e\tau} \\ \sim & \eta c_{12}^2 + \hat{A} \hat{\varepsilon}_{\mu\mu} & \hat{A} \hat{\varepsilon}_{\mu\tau} \\ \sim & \sim & \hat{A} \hat{\varepsilon}_{\tau\tau} \end{pmatrix}, \quad (32)$$

with ‘ \sim ’ denoting the conjugate elements and $\hat{\varepsilon}_{\alpha\beta} = (V_\delta^\dagger O_{23}^T \cdot \varepsilon \cdot O_{23} V_\delta)_{\alpha\beta}$. Since $M^{(0)}$ is diagonal at zeroth order, we have $\hat{V}^{(0)} = I$. Then, the first order corrections are given by

$$\lambda_i^{(1)} = M_{ii}^{(1)}, \quad (33)$$

and

$$\hat{V}_i^{(1)} = \sum_{j \neq i} \frac{M_{ji}^{(1)}}{\lambda_i^{(0)} - \lambda_j^{(0)}} \hat{V}_j^{(0)}. \quad (34)$$

Thus, the effective masses and mixing matrix are given by $\tilde{m}_i^2 \simeq \Delta_{31}(\lambda_i^{(0)} + \lambda_i^{(1)})$ and $\tilde{V} \simeq O_{23} V_\delta (\hat{V}^{(0)} + \hat{V}^{(1)})$, respectively. Finally, inserting Eq. (32) into Eqs. (33) and (34), we arrive

at mappings for the effective mass squares

$$\tilde{m}_1^2 \simeq \Delta_{31} \left(\hat{A} + \eta s_{12}^2 + \hat{A} \varepsilon_{ee} \right) , \quad (35)$$

$$\tilde{m}_2^2 \simeq \Delta_{31} \left[\eta c_{12}^2 - \hat{A} s_{23}^2 (\varepsilon_{\mu\mu} - \varepsilon_{\tau\tau}) - \hat{A} s_{23} c_{23} (\varepsilon_{\mu\tau} + \varepsilon_{\mu\tau}^*) + \hat{A} \varepsilon_{\mu\mu} \right] , \quad (36)$$

$$\tilde{m}_3^2 \simeq \Delta_{31} \left[1 + \hat{A} \varepsilon_{\tau\tau} + \hat{A} s_{23}^2 (\varepsilon_{\mu\mu} - \varepsilon_{\tau\tau}) + \hat{A} s_{23} c_{23} (\varepsilon_{\mu\tau} + \varepsilon_{\mu\tau}^*) \right] , \quad (37)$$

the effective mixing matrix elements,

$$\tilde{V}_{e2} \simeq \frac{\eta s_{12} c_{12}}{\hat{A}} + c_{23} \varepsilon_{e\mu} - s_{23} \varepsilon_{e\tau} , \quad (38)$$

$$\tilde{V}_{e3} \simeq \frac{s_{13} e^{-i\delta}}{1 - \hat{A}} + \frac{\hat{A} (s_{23} \varepsilon_{e\mu} + c_{23} \varepsilon_{e\tau})}{1 - \hat{A}} , \quad (39)$$

$$\tilde{V}_{\mu 2} \simeq c_{23} + s_{23}^2 c_{23} \hat{A} (\varepsilon_{\tau\tau} - \varepsilon_{\mu\mu}) + s_{23} \hat{A} (s_{23} \varepsilon_{\mu\tau} - c_{23}^2 \varepsilon_{\mu\tau}^*) , \quad (40)$$

$$\tilde{V}_{\mu 3} \simeq s_{23} + \hat{A} [s_{23} (\varepsilon_{\mu\mu} - \varepsilon_{\tau\tau}) + c_{23} \varepsilon_{\mu\tau} - s_{23}^2 c_{23} (\varepsilon_{\mu\tau} + \varepsilon_{\mu\tau}^*) + s_{23}^3 (\varepsilon_{\tau\tau} - \varepsilon_{\mu\mu})] , \quad (41)$$

and the effective Jarlskog parameter

$$\begin{aligned} \tilde{J} = & \frac{s_{13} s_{23} \left(\eta s_{\delta} c_{12} c_{23} s_{12} + \hat{A} s_{\delta + \phi_{e\mu}} c_{23}^2 |\varepsilon_{e\mu}| - \hat{A} s_{\delta + \phi_{e\tau}} c_{23} s_{23} |\varepsilon_{e\tau}| \right)}{(\hat{A} - 1) \hat{A}} \\ & + \frac{s_{23} \left(s_{\phi_{e\mu} - \phi_{e\tau}} c_{23} |\varepsilon_{e\mu}| |\varepsilon_{e\tau}| \hat{A}^2 - \eta s_{\phi_{e\mu}} c_{12} c_{23} s_{12} s_{23} |\varepsilon_{e\mu}| \hat{A} - \eta s_{\phi_{e\tau}} c_{12} s_{12} c_{23}^2 |\varepsilon_{e\tau}| \hat{A} \right)}{(\hat{A} - 1) \hat{A}} , \quad (42) \end{aligned}$$

where the $\phi_{\alpha\beta}$'s are the phases associated with the complex NSI parameters $\varepsilon_{\alpha\beta}$ and the $s_{\phi_{\alpha\beta}}$'s are the corresponding sine functions. The above mappings can be transferred into mappings between mixing angles straightforwardly, i.e., we have approximately $\tilde{s}_{13} \simeq |\tilde{V}_{e3}|$, $\tilde{s}_{12} \simeq |\tilde{V}_{e2}|$, and $\tilde{s}_{23} \simeq |\tilde{V}_{\mu 3}|$. Equations (35)-(42) are our main results for the approximate analytical mappings.

Some discussions are in order:

- In the limit $\varepsilon_{\alpha\beta} \rightarrow 0$, it is interesting to observe that our results coincide with the mapping results in Ref. [58] when evaluated at the same order of perturbation theory. In fact, expanding Eqs. (27a)-(27c) of Ref. [58] in η and s_{13} (which means that the \hat{C} parameter appearing there equals $1 - \hat{A}$), and retaining terms up to first order in these small parameters, we can easily check that they reduce to

$$\tilde{s}_{13} = \frac{s_{13}}{1 - \hat{A}} , \quad (43)$$

$$\tilde{s}_{23} = s_{23} , \quad (44)$$

$$\tilde{s}_{12} = \frac{\eta}{\hat{A}} c_{12} s_{12} , \quad (45)$$

which are in agreement with our Eqs. (38)-(41) evaluated at $\varepsilon_{\alpha\beta} = 0$. In addition, from Eq. (43), it is worth noticing that the mixing parameter s_{13} is strongly modified by matter effects when $0 < \hat{A} \neq 1$, otherwise the resonance $\hat{A} = 1$ is at work and the mapping procedure adopted in this paper is not valid.

- As shown in Eq. (29), the orthogonal matrix O_{23} commutes with the standard matter potential. Hence, in the case of vanishing θ_{13} and NSIs, Eq. (8) can be rewritten as

$$\tilde{H} = \frac{\Delta_{31}}{2E} O_{23} \left[O_{12} \cdot \text{diag}(0, \eta, 1) \cdot O_{12}^T + \text{diag}(\hat{A}, 0, 0) \right] O_{23}^T, \quad (46)$$

where the CP violating phase δ loses its meaning and does not appear. An evident conclusion deduced from Eq. (46) is that, if $\theta_{13} = 0$, the standard matter effects only contribute to the mixing angle θ_{12} . Both θ_{13} and θ_{23} as well as Δ_{31} will keep their vacuum values in matter. However, when the NSIs are taken into account, the situation will be quite different. A non-zero $\tilde{\theta}_{13}$ will emerge in general, $\tilde{\theta}_{23}$ will deviate from its maximal value $\pi/4$, and a non-trivial CP violating phase $\tilde{\delta}$ may also exist.

- As already noticed above, the mapping for θ_{12} shows an unphysical divergence for $\hat{A} \rightarrow 0$ or $\hat{A} \rightarrow 1$, and the vacuum results cannot be reproduced, a well-known consequence of the perturbative approach adopted in the mapping procedure. Thus, degenerate perturbation theory should be elaborated on around these two singularities.
- Except from $\varepsilon_{e\mu}$ and $\varepsilon_{e\tau}$, it can also be very clearly seen that contributions to \tilde{s}_{13} from all the other NSI parameters are all suppressed. Since the present experimental bound on $\varepsilon_{e\mu}$ is rather stringent [43], we conclude that $\varepsilon_{e\tau}$ is the most significant NSI parameter to be taken into account for $\tilde{\theta}_{13}$. As for $\tilde{\theta}_{23}$, NSI corrections are relatively mild unless very high-energy regions are considered.
- The matrix elements $|\tilde{V}_{\mu 3}|$, $|\tilde{V}_{\tau 3}|$, $|\tilde{V}_{\mu 1}|$, and $|\tilde{V}_{\tau 1}|$ are not modified by $\varepsilon_{e\tau}$.

V. APPLICATIONS

We now proceed to numerically illustrate (using normal mass hierarchy, i.e., $\eta \simeq +0.032$) the NSI corrections to the leptonic mixing parameters and the neutrino oscillations probabilities based on our model independent results obtained in Secs. III and IV. We first consider

the exact results for mixing matrix elements, and combinations of them, as obtained applying Eq. (20). This is an important point, since both mixing angles and the Jarlskog parameter depend on the modified behavior of the effective matrix elements [see Eqs. (22) and (26)] due to matter effects and non-standard physics. We then focus on the importance of the NSI effects on θ_{13} and θ_{23} in correcting their tri-bimaximal mixing values (i.e., $\theta_{13} = 0$ and $\theta_{23} = \pi/4$) [59, 60]. Finally, in order to show the goodness of our approximate results for the effective mixing angles, we compare the exact $\nu_e \rightarrow \nu_\mu$, $\nu_e \rightarrow \nu_\tau$, and $\nu_\mu \rightarrow \nu_\tau$ oscillation probabilities obtained including the NSI effects with those derived using Eqs. (38)-(41) for the effective mixing angles.

A. NSI corrections to the leptonic mixing matrix

The effective leptonic mixing matrix can be reconstructed directly from Eq. (20). For $\alpha = \beta$, we obtain the expressions of the matrix elements $|\tilde{V}_{\alpha i}|$, whereas for $\alpha \neq \beta$, we obtain the sides of unitarity triangles $\tilde{V}_{\alpha i} \tilde{V}_{\beta i}^*$. The numerical results are presented in Fig. 1. In our numerical calculations, we take the central values of the neutrino mass-squared differences ($\Delta_{21} = 7.65 \times 10^{-5} \text{ eV}^2$, $\Delta_{31} = 2.4 \times 10^{-3} \text{ eV}^2$) and the leptonic mixing angles ($\theta_{12} = 33.5^\circ$, $\theta_{23} = 45^\circ$, $\theta_{13} = 0$) obtained in a global analysis of the presently available neutrino oscillation data [57]. Here, just as an example, we choose $\varepsilon_{e\tau}$ as the only non-vanishing NSI parameter. For comparison, we also show the results without including NSIs. In particular, for higher neutrino beam energies, the NSI corrections are remarkable.

First, we can observe that the energy dependence of the matrix elements can be easily read off from the approximate relations in Eqs. (38)-(41), since the matter parameter $A \sim E$.² Thus, for example, the fact that $|\tilde{V}_{e2}|$ is predicted to decrease with increasing neutrino energy is confirmed in the first panel of the fourth row in Fig. 1. Moreover, the singularity for matrix elements around $E \sim 10 \text{ GeV}$ (see panels in the first and third rows) clearly corresponds to the resonance at $\hat{A} \sim 1$, which can be understood investigating the perturbative results in Eqs. (38)-(41). Note that, for anti-neutrinos, since the sign in front of \hat{A} is negative, such a singularity should not appear. In addition, the relation $|\tilde{V}_{ei} \tilde{V}_{\mu i}^*| \simeq |\tilde{V}_{ei} \tilde{V}_{\tau i}^*|$ holds quite well, which is an obvious consequence of the $\mu - \tau$ symmetry in the genuine neutrino mass matrix.

² The matrix elements that are not quoted in Eqs. (38)-(41) can be obtained using unitarity relations.

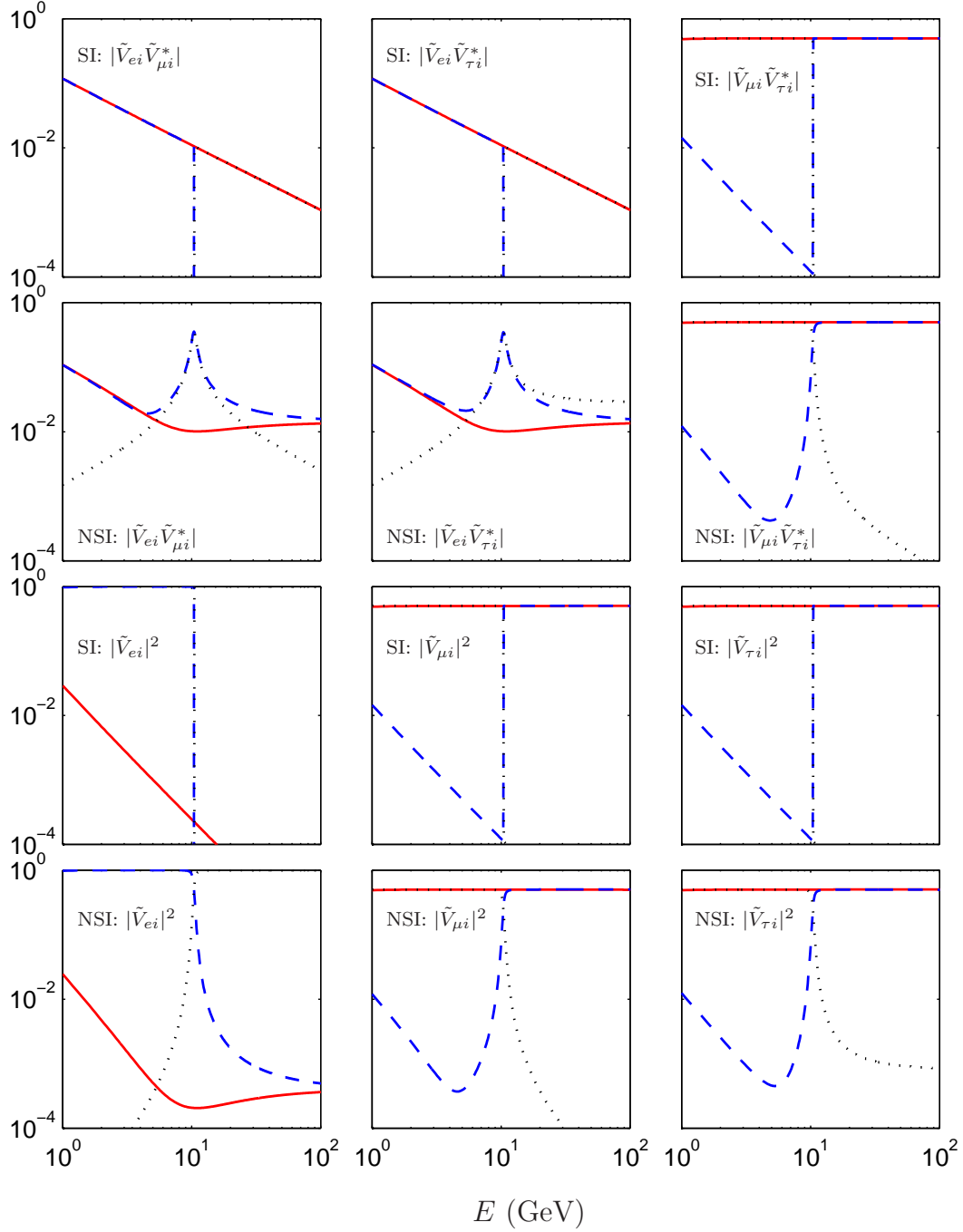


FIG. 1: Illustrative plots for the effective matrix elements $|\tilde{V}_{\alpha i} \tilde{V}_{\beta i}^*|$ (first and second rows) and $|\tilde{V}_{\alpha i}|^2$ (third and fourth rows) as a function of the neutrino energy E . Here the solid, dashed, and dotted curves correspond to $i = 1, 2, 3$, respectively. The first and third rows show the results without including NSIs (labeled SI), while the second and fourth rows are those including NSIs. We use the representative value $\text{Re}(\varepsilon_{e\tau}) = \text{Im}(\varepsilon_{e\tau}) = 0.02$, with all other $\varepsilon_{\alpha\beta}$ being zero.

This can be seen comparing the first and second panels of the second row for any value of the index i . In the same panels, at energies $E \sim 4$ GeV, $\tilde{V}_{ei}\tilde{V}_{\mu i}^*$ and $\tilde{V}_{ei}\tilde{V}_{\tau i}^*$ ($i = 1, 2, 3$) are comparable to each other, and thus, the unitarity triangle built with these sides takes a nearly equilateral form with three nearly degenerate inner angles. Such an equilateral form is destroyed when increasing the energy. Similarly, $|\tilde{V}_{\mu 1}\tilde{V}_{\tau 1}^*|$ is rather stable against matter corrections and NSI effects, which also reflects the stabilization of $\tilde{\theta}_{23}$. As for the matrix elements, $|\tilde{V}_{\mu 1}|$ and $|\tilde{V}_{\tau 1}|$ are not sensitive to $\varepsilon_{e\tau}$, which is also in agreement with our approximate mappings.

B. NSI corrections to the mixing angles

A crucial goal of future neutrino facilities is to measure the smallest leptonic mixing angle θ_{13} in order to extract information on leptonic CP violation. However, it has been pointed out that NSIs may play a very important role for mimicking effects on θ_{13} and leptonic CP violation, especially in the case of a small θ_{13} [61]. It is then quite important to analyze in detail these effects in order to be able to disentangle genuine θ_{13} effects from new physics-induced ones at future neutrino facilities.

On the other hand, the question of whether the leptonic mixing angle $\tilde{\theta}_{23}$ is exactly maximal or not is quite relevant, especially from the model builders' point of view: in fact, many models presented in the literature predict θ_{23} being (almost) maximal and the understanding of the flavor problem strongly relies on the knowledge on the value of θ_{23} to be as accurate as possible. Thus, it is very important to investigate the possible NSI corrections to θ_{13} and the maximal mixing pattern in the $\mu - \tau$ sector.

According to Eqs. (38)-(41), the most relevant NSI parameter for $\tilde{\theta}_{13}$ is $\varepsilon_{e\tau}$ (since the upper bound on $\varepsilon_{e\mu}$ is rather stringent), whereas for $\tilde{\theta}_{23}$ $\varepsilon_{\mu\tau}$, $\varepsilon_{\mu\mu}$ and $\varepsilon_{\tau\tau}$ contribute. Notice that, in the latter case for maximal mixing ($\theta_{23} = 45^\circ$), a typical feature is that the vacuum Hamiltonian takes on a $\mu - \tau$ symmetric form, namely, H is invariant under the exchange of μ and τ indices. Hence, if NSIs possess a similar $\mu - \tau$ symmetric form (i.e., $\varepsilon_{e\mu} = \varepsilon_{e\tau}$ and $\varepsilon_{\mu\mu} = \varepsilon_{\tau\tau}$), the $\mu - \tau$ symmetry exists in the effective Hamiltonian \tilde{H} , and the effective mixing angle $\tilde{\theta}_{23}$ will not be affected by matter effects. As a consequence, $\varepsilon_{\mu\tau}$ itself does not contribute to $\tilde{\theta}_{23}$ if all the other NSI parameters are zero.

In the upper plots of Fig. 2, we show the non-vanishing $\tilde{\theta}_{13}$ generated by the NSIs [com-

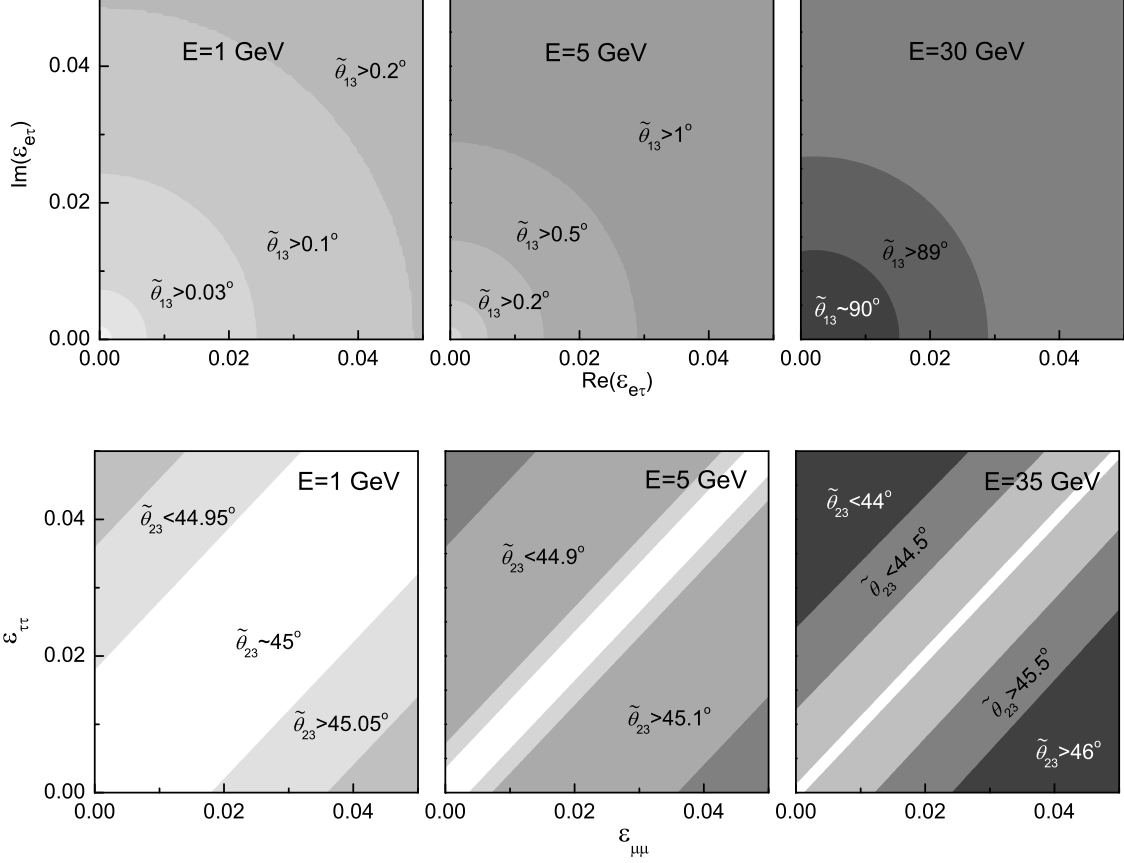


FIG. 2: Dependence of the mixing angles $\tilde{\theta}_{13}$ and $\tilde{\theta}_{23}$ on the NSI parameters for three representative values of the neutrino energy: $E = 1, 5,$ and 30 (35) GeV , which roughly correspond to the ν_e and ν_μ mean energies at a 50 GeV neutrino factory. The vacuum value of θ_{13} is fixed to be zero, whereas we assume maximal mixing for θ_{23} . In each plot, the darker the region, the larger the deviation of $\tilde{\theta}_{13}$ and $\tilde{\theta}_{23}$ from their vacuum values. Only the labeled NSI parameters are non-vanishing in each plot.

puted using our exact formula given in Eq. (20)]. One can observe that $\tilde{\theta}_{13}$ is quite sensitive to $\epsilon_{e\tau}$. In the case of $E = 30$ GeV , $\tilde{\theta}_{13}$ may acquire a very sizable value close to 90° . This is due to the reordering of the eigenvalues \tilde{m}_1 and \tilde{m}_3 when $E \gtrsim 10$ GeV . If we keep the order of eigenvalues in the form of $\text{diag}(\tilde{m}_1^2, \tilde{m}_2^2, \tilde{m}_3^2)$, a shift of $\pi/2$ has to be added to $\tilde{\theta}_{13}$. In the lower plots of Fig. 2, we show the corrections from $\epsilon_{\mu\mu}$ and $\epsilon_{\tau\tau}$ to θ_{23} , assuming the vacuum value $\theta_{23} = \pi/4$. Our numerical results indicate that there are no sizable corrections to the mixing angle θ_{23} , and even in the high-energy region, $\tilde{\theta}_{23}$ should not deviate from its maximal value by more than a few degrees. We also find that the $\epsilon_{\mu\mu} - \epsilon_{\tau\tau}$ contributions

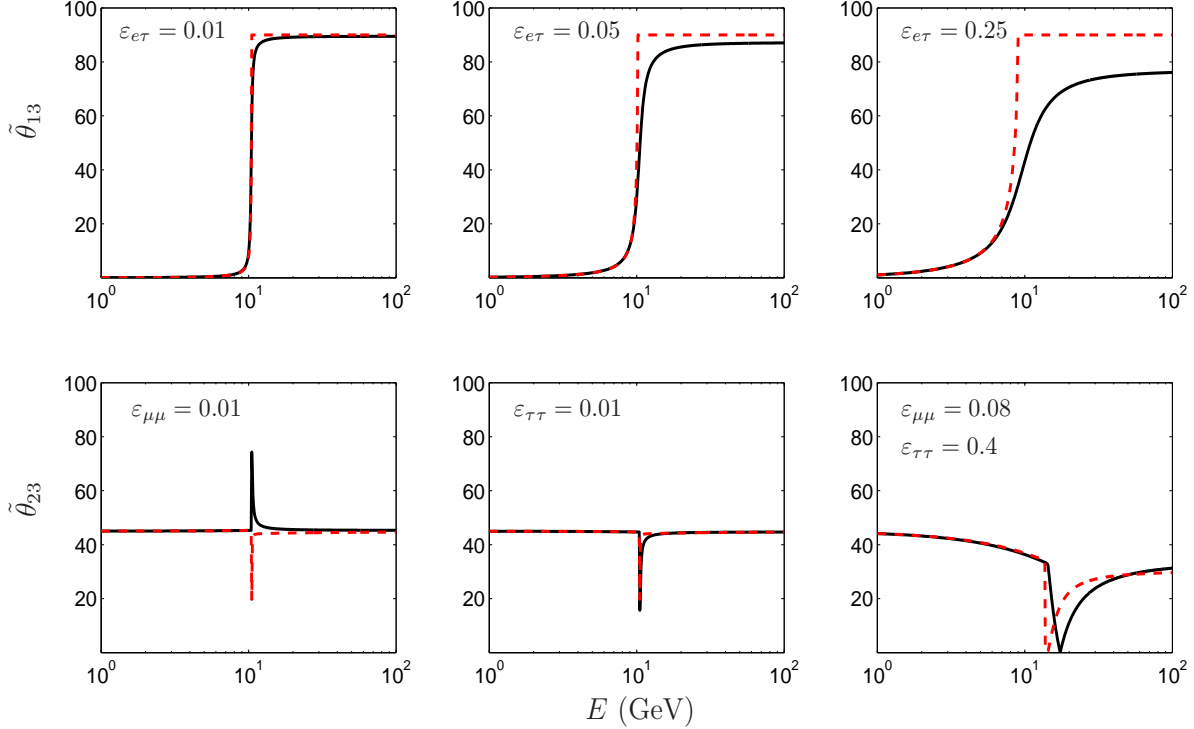


FIG. 3: Neutrino energy dependence of the effective mixing angles ($\tilde{\theta}_{13}$ and $\tilde{\theta}_{23}$). Solid curves correspond to exact numerical results, whereas the dashed ones are computed using our approximate mappings. The non-vanishing NSI parameters have been labeled in each plot.

are symmetric with respect to the $\varepsilon_{\mu\mu} = \varepsilon_{\tau\tau}$ axis up to a minus sign, since an addition to one of the parameters could as well be made to the other one.

It is interesting to observe that the main features of the previous *exact* results can also be captured from our approximate mappings in Eqs. (38)-(41). To illustrate this point, we show the dependence of $\tilde{\theta}_{13}$ and $\tilde{\theta}_{23}$ on the neutrino energy in Fig. 3, for different values of the relevant NSI parameters, according to our foregoing discussions. Solid curves correspond to exact results obtained using Eq. (20), whereas dashed ones represent our perturbative mappings. In the first row, we can appreciate how the dependence of $\tilde{\theta}_{13}$ on $\varepsilon_{e\tau}$ is well described by our perturbative result in Eq. (38), unless $\varepsilon_{e\tau}$ assumes a very large value, close to its upper bound [30]. In addition, notice that the increase of $\tilde{\theta}_{13}$ corresponds to reordering the eigenvalues for energies around 10 GeV. In the second row, we analyze the behavior of $\tilde{\theta}_{23}$, for different values of the relevant parameters $\varepsilon_{\mu\mu}$ and $\varepsilon_{\tau\tau}$. In particular, in the first and

second panels, we choose only one of them being different from zero (and equal to 0.01), whereas in the last one, we allow both of them to assume larger values ($\varepsilon_{\mu\mu} = 0.08$ and $\varepsilon_{\tau\tau} = 0.4$). The agreement between our calculation and the exact evaluation of $\tilde{\theta}_{23}$ is quite good, also in predicting the location of the resonance.

Finally, we comment on the fact that $\tilde{\theta}_{12}$ is dramatically suppressed by matter effects, as shown in Eq. (38). However, since long-baseline neutrino oscillation experiments are not very sensitive to this angle, we will not perform a detailed analysis here. The conclusions made above about the dependence of the effective angles on the NSI parameters apply as well to the case of anti-neutrinos in matter and we will not perform such a redundant analysis here.

C. NSI corrections to the neutrino oscillation probabilities

Until now we have described the relevant features of new physics effects on the matrix elements of the leptonic mixing matrix. In what follows, we study the dependence of the transition probabilities on the NSI parameters, for different choices of neutrino energies and baselines. In particular, we focus on the *golden channel* $\nu_e \rightarrow \nu_\mu$ [62] and the CP asymmetries derived from it, the *silver channel* $\nu_e \rightarrow \nu_\tau$ [63, 64], and the so-called *discovery channel* $\nu_\mu \rightarrow \nu_\tau$, which is thought to be the best channel for searching for new physics [65]. We also show how the relevant features of the transition probabilities are well reproduced computing them by inserting Eqs. (38)-(41) into Eq. (11).

In Fig. 4, we show the transition probability $P(\nu_e \rightarrow \nu_\mu)$ as a function of the neutrino energy for three different baseline setups: $L = 700$ km (around the scope of MINOS [10] and OPERA [66]), $L = 3000$ km, and $L = 7000$ km (for the two detector setup of a neutrino factory). The input parameters are the same as those in Fig. 1. In each panel, the solid curves denote the exact numerical results, the dashed curves correspond to results derived from our approximate mappings and, to highlight the effects of the NSI parameters, the dotted curves represent the probability without including NSIs. We can observe that our approximate mappings given in Sec. IV agree with the exact numerical results to an extremely good precision. Similar to the plots of the mixing parameters, a singularity exists around $E \sim 10$ GeV due to the limitation of non-degenerate perturbation theory that we have elaborated. For smaller θ_{13} , the probability is more sensitive to the NSI effects, and

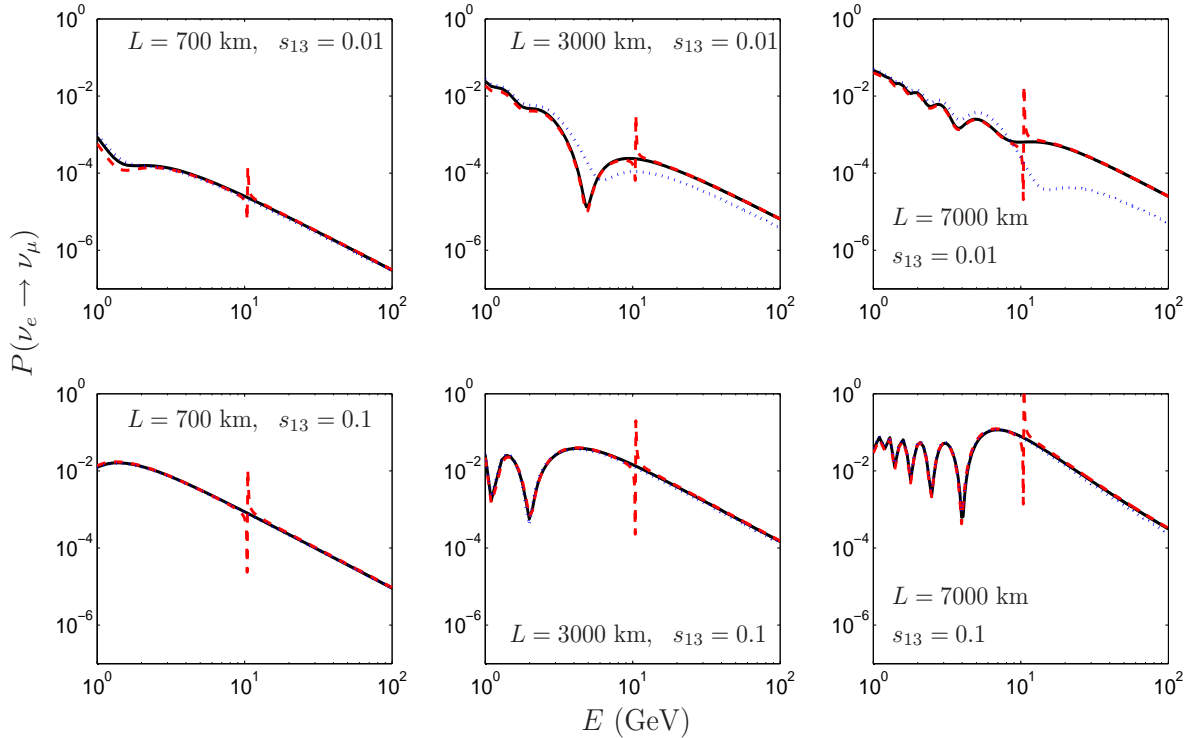


FIG. 4: Neutrino oscillation probabilities for the $\nu_e \rightarrow \nu_\mu$ channel as a function of the neutrino energy E . The baseline lengths and values of s_{13} have been labeled in each plot. Here, we set $\delta = \pi/2$ and only $\varepsilon_{e\tau} = 0.01$ is allowed to be non-vanishing. The solid curves denote the exact numerical results. The dashed curves correspond to results derived from our approximate mappings, and for comparison, the dotted curves are shown to illustrate probabilities without including NSIs.

thus, longer baseline lengths are more favored for the purpose of searching for new physics effects.

The experimentally measured CP asymmetry in the golden channel, which is usually defined as

$$\mathcal{A}_{CP} = \frac{P(\nu_e \rightarrow \nu_\mu) - P(\bar{\nu}_e \rightarrow \bar{\nu}_\mu)}{P(\nu_e \rightarrow \nu_\mu) + P(\bar{\nu}_e \rightarrow \bar{\nu}_\mu)}, \quad (47)$$

is illustrated in Fig. 5 for the same baseline setup. Again, our approximate mappings are valid in a large range of beam energies. At higher energies, the CP asymmetries are dramatically affected by NSIs, i.e., the values of \mathcal{A}_{CP} , which are calculated without taken into account NSI effects, may go to divergent directions.

In Figs. 6 and 7, we repeat the same exercise on the neutrino oscillation probabilities and CP asymmetries, but instead as a function of the baseline length and for two fixed

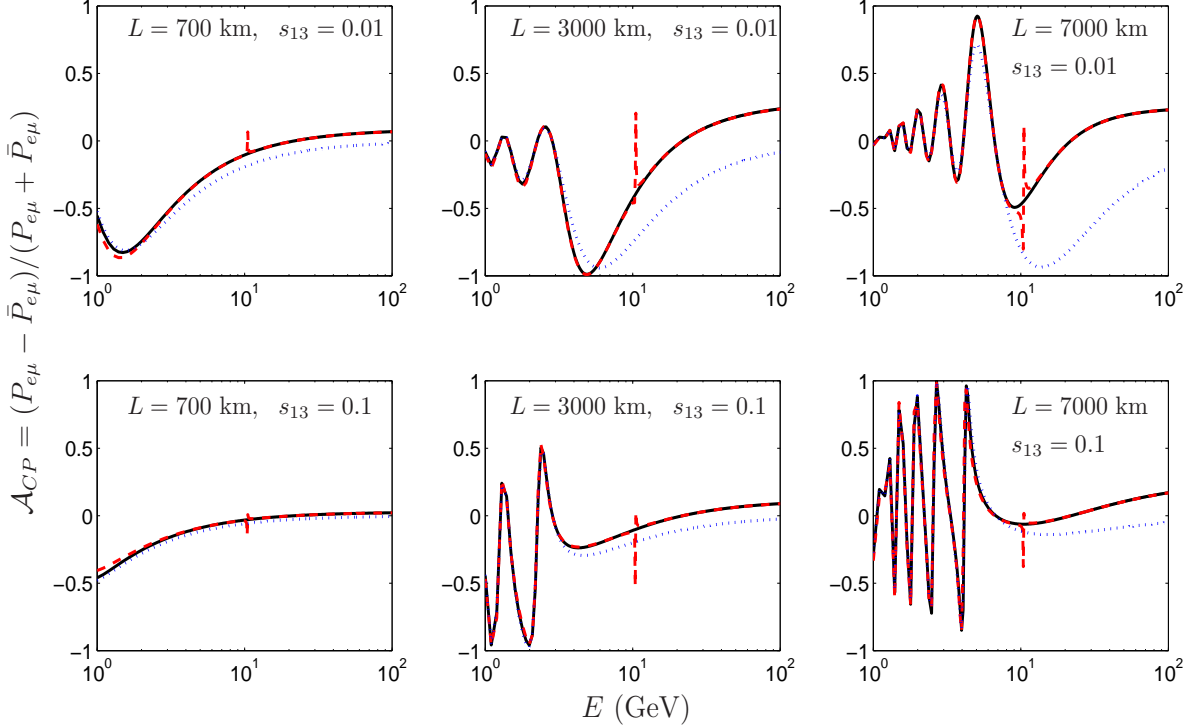


FIG. 5: CP asymmetry \mathcal{A}_{CP} derived from the $\nu_e \rightarrow \nu_\mu$ channel. The values of the mixing parameters as well as those of the baselines and neutrino energies are the same as in Fig. 4. The solid curves denote the exact numerical results, the dashed curves correspond to results derived from our approximate mappings, and the dotted curves show the probabilities without including NSIs.

value of the neutrino energy $E = 5$ GeV and $E = 30$ GeV. It can be clearly seen that for smaller θ_{13} and lower beam energy, new physics effects play a significant role around $L \sim 3000$ km, which sheds some light on future beta beam experiments. For higher energy experiments, i.e., a neutrino factory, a far detector with relatively longer baseline length should be important to constrain NSI effects. In both figures, one can appreciate how the probabilities computed using our approximations for the effective mixing angles are in very good agreement with the exact results.

Finally, we illustrate the application of our analytical expressions for the $\nu_e \rightarrow \nu_\tau$ and $\nu_\mu \rightarrow \nu_\tau$ channels in Fig. 8. For comparison, we also show the maximal NSI corrections by setting all the NSI parameters at their upper bounds given in Ref. [30]. One can observe that NSI corrections to these two channels are not remarkable if the corresponding $\varepsilon_{\alpha\beta}$'s are chosen to be a few percent. However, increasing the NSI parameters, the NSI effects become

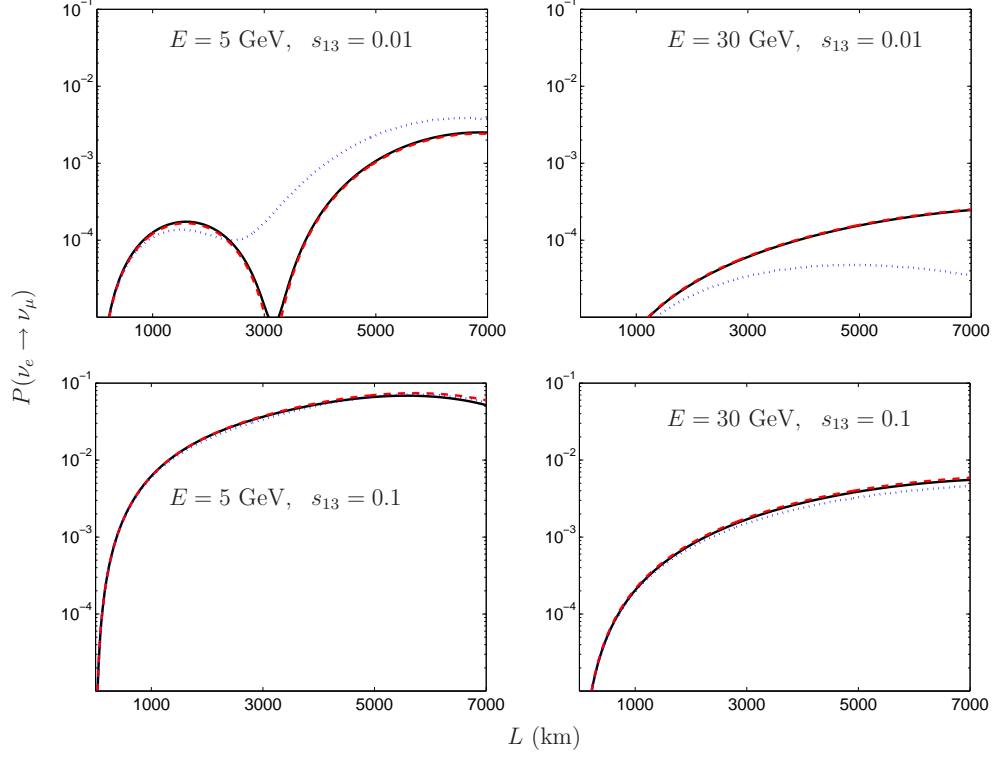


FIG. 6: Transition probability $P(\nu_e \rightarrow \nu_\mu)$ as a function of the baseline length L . Here, $\varepsilon_{e\tau} = 0.01$ and $\delta = \pi/2$ are adopted, and the neutrino beam energies have been labeled in each plot. The solid and dotted curves denote the exact numerical results with and without NSIs, respectively. Probabilities calculated using our approximate mappings are shown as dashed curves.

more significant, in particular for the $\nu_e \rightarrow \nu_\tau$ channel. The upper plots in Fig. 8 indicate that our approximate mappings are not quite valid for relatively longer baseline lengths. This is due to the fact that our expansions are performed according to small $\varepsilon_{\alpha\beta}$'s and cannot be extended to the regions of sizable NSI parameters. As discussed in the introduction, if NSIs are related to some underlying new physics, they should be attributed to next-to-leading order effects and not deviate much from zero. In this sense, our approximate mappings are quite realistic and should be very helpful for both phenomenological studies and model buildings.

Since the analyses above certainly depend on the input NSI parameters, they mainly serve as illustrations. However, our analytical results are model independent. Thus, they are hoped to be very useful for a general study of NSI effects in future experiments. The transparent mappings also manifest the underlying correlations between leptonic mixing

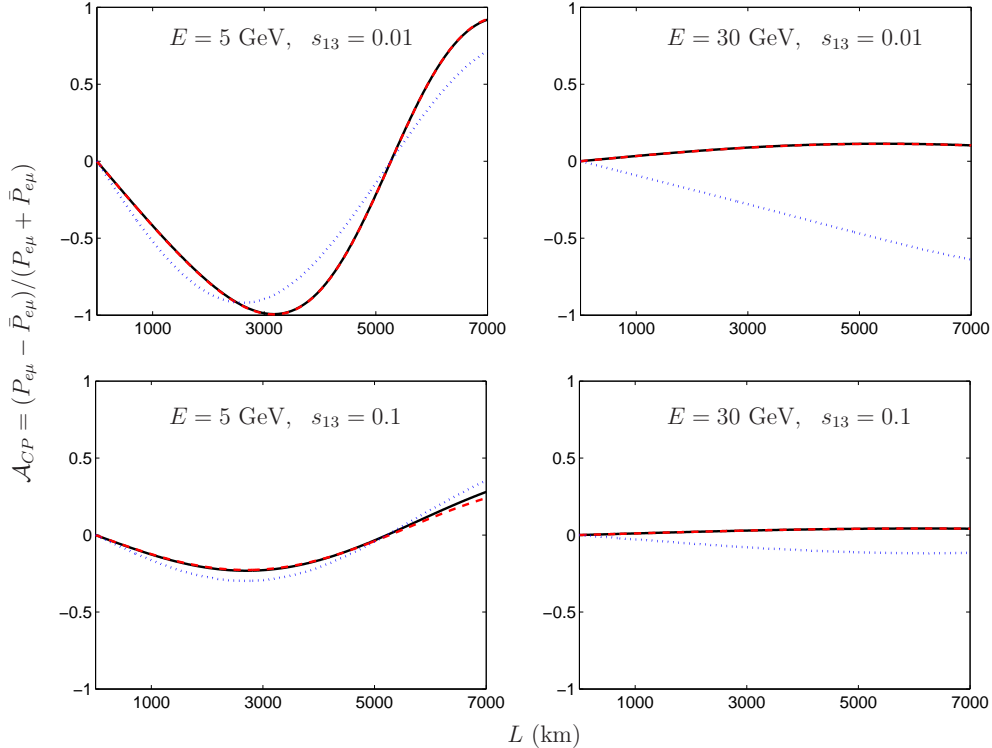


FIG. 7: CP asymmetries as a function of the baseline lengths. Here, $\varepsilon_{e\tau} = 0.01$ and the neutrino beam energies have been shown in each plot. The solid and dotted curves denote the exact numerical results with and without NSIs, respectively. Dashed curves denote \mathcal{A}_{CP} calculated using the approximate mappings.

parameters and NSIs in a very legible way.

VI. SUMMARY

In this work, we have developed both exact and approximate mappings between the leptonic mixing matrix in vacuum and in matter in the presence of NSIs. A full set of sum rules between fundamental mixing parameters and the corresponding effective ones in matter have been derived. By using these sum rules, exact and model independent analytical mappings between the mixing matrix elements $\tilde{V}_{\alpha i}$ and $V_{\alpha i}$ have been established, and in turn using these mappings, the moduli of the mixing matrix elements and the sides of unitarity triangles can be immediately figured out. Besides the exact expressions for the mixing parameters, we have also derived approximate parameter mappings based on series

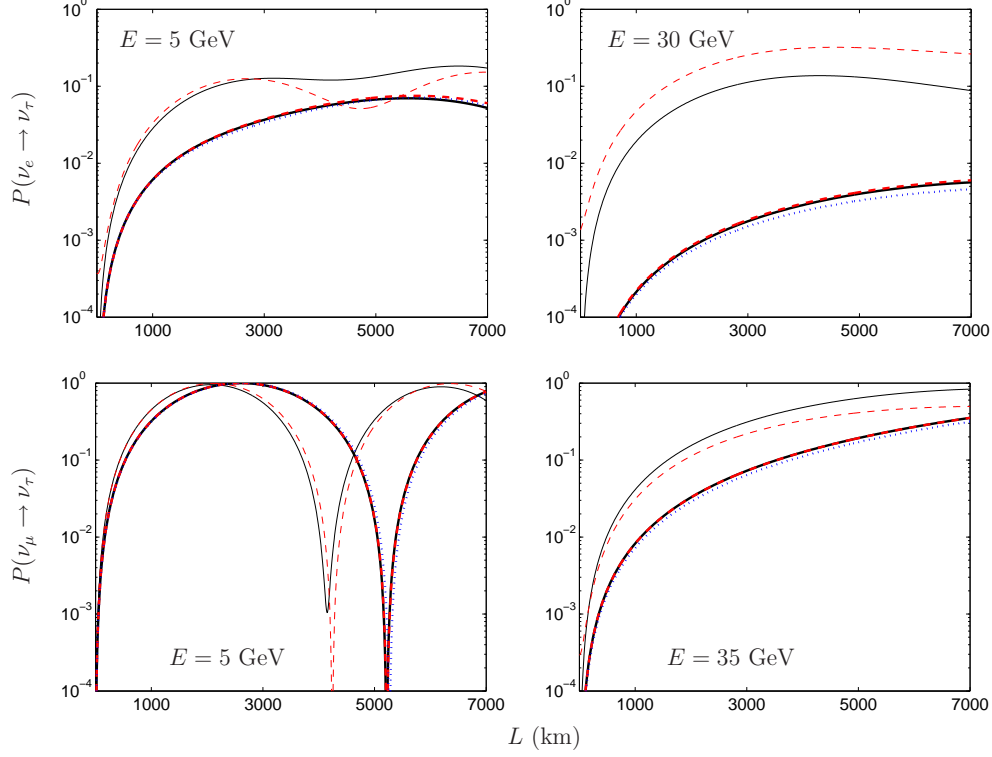


FIG. 8: Transition probabilities for the $\nu_e \rightarrow \nu_\tau$ and $\nu_\mu \rightarrow \nu_\tau$ channels as a function of the baseline length L . Different setups of NSI parameters are considered: (a) for the $\nu_e \rightarrow \nu_\tau$ channel, we choose $\varepsilon_{e\tau} = 0.01$, and for the $\nu_\mu \rightarrow \nu_\tau$ channel, we choose $\varepsilon_{\mu\mu} = \varepsilon_{\mu\tau} = \varepsilon_{\tau\tau} = 0.01$. Here, thick solid and dashed curves correspond to the exact numerical results and our approximate mappings, respectively; (b) NSI parameters are at their upper bounds computed in Ref. [30] with thin solid and dashed curves corresponding to the exact numerical results and our approximate mappings, respectively. Dotted curves denote the numerical results without including NSIs, and they are unique in each channel.

expansions in the small parameters η , s_{13} , and $\varepsilon_{\alpha\beta}$. We have then performed a detailed numerical analysis of the application and validity of our parameter mappings. In particular, we have concentrated on the mimicking effects of NSIs on the mixing angle θ_{13} and on the deviation of the mixing angle θ_{23} from maximal mixing. Furthermore, we have studied in detail how the $\varepsilon_{\alpha\beta}$'s affect the transition probabilities of the $\nu_e \rightarrow \nu_\mu$, $\nu_e \rightarrow \nu_\tau$, and $\nu_\mu \rightarrow \nu_\tau$ channels. We have found that the exact parameter mappings are very useful in obtaining exact results for the mixing parameters and transition probabilities, and our perturbative parameter mappings also describe quite well all the relevant features of these quantities.

Note that our analytical analysis is independent of any specific model or assumptions on the configuration of NSI parameters. In conclusion, the outstanding feature of our parameter mappings is that they reveal the underlying correlations between NSI effects and neutrino mixing parameters in a highly straightforward way, and they are very practical and useful for the study of NSIs in future long-baseline neutrino oscillation experiments. It also makes sense to note that the calculation procedures we have employed in the present work can also be applied to the picture of non-unitary leptonic mixing [47], which will be elaborated on elsewhere.

Acknowledgments

We would like to thank Mattias Blennow for useful discussions. This work was supported by the Royal Swedish Academy of Sciences (KVA) [T.O.], the Göran Gustafsson Foundation [H.Z.], and the Swedish Research Council (Vetenskapsrådet), contract no. 621-2008-4210 [T.O.]. D.M. acknowledges partial financial support from the Ministry of University and Scientific Research of Italy, through the 2007-08 COFIN program.

APPENDIX A: CALCULATIONS OF EFFECTIVE MASSES

To calculate the explicit expressions of \tilde{m}_i , the cubic roots of the characteristic polynomial of Eq. (8) are involved. We follow the method given in Ref. [51] and define the so-called elementary symmetric polynomials [67, 68]:

$$c_0 = \tilde{H}_{ee} \left| \tilde{H}_{\mu\tau} \right|^2 + \tilde{H}_{\mu\mu} \left| \tilde{H}_{e\tau} \right|^2 + \tilde{H}_{\tau\tau} \left| \tilde{H}_{e\mu} \right|^2 - 2\text{Re}(\tilde{H}_{e\mu} \tilde{H}_{\mu\tau} \tilde{H}_{\tau e}) - \tilde{H}_{ee} \tilde{H}_{\mu\mu} \tilde{H}_{\tau\tau} , \quad (\text{A1})$$

$$c_1 = \tilde{H}_{ee} \tilde{H}_{\mu\mu} + \tilde{H}_{ee} \tilde{H}_{\tau\tau} + \tilde{H}_{\mu\mu} \tilde{H}_{\tau\tau} - \left| \tilde{H}_{e\mu} \right|^2 - \left| \tilde{H}_{\mu\tau} \right|^2 - \left| \tilde{H}_{e\tau} \right|^2 , \quad (\text{A2})$$

$$c_2 = -\tilde{H}_{ee} - \tilde{H}_{\mu\mu} - \tilde{H}_{\tau\tau} . \quad (\text{A3})$$

It is easy to check that the relations $c_2 = -\sum_i \tilde{m}_i^2/(2E)$, $c_1 = \sum_{i<j} \tilde{m}_i^2 \tilde{m}_j^2/(2E)^2$, and $c_0 = -\prod_i \tilde{m}_i^2/(2E)^3$ are satisfied. By incorporating the definitions above, the mass squared eigenvalues can be computed as

$$\frac{\tilde{m}_1^2}{2E} = \frac{2}{3} \sqrt{p} \cos \left[\frac{1}{3} \arctan \left(\frac{\sqrt{p^3 - q^2}}{q} \right) + \frac{2\pi}{3} \right] - \frac{1}{3} c_2 , \quad (\text{A4})$$

$$\frac{\tilde{m}_2^2}{2E} = \frac{2}{3} \sqrt{p} \cos \left[\frac{1}{3} \arctan \left(\frac{\sqrt{p^3 - q^2}}{q} \right) - \frac{2\pi}{3} \right] - \frac{1}{3} c_2 , \quad (\text{A5})$$

$$\frac{\tilde{m}_3^2}{2E} = \frac{2}{3} \sqrt{p} \cos \left[\frac{1}{3} \arctan \left(\frac{\sqrt{p^3 - q^2}}{q} \right) \right] - \frac{1}{3} c_2 , \quad (\text{A6})$$

where $p = c_2^2 - 3c_1$ and $q = -27c_0/2 - c_2^3 + 9c_1c_2/2$. As a natural consequence, the effective mass eigenvalues in matter are only related with the neutrino mass squared differences but not the absolute neutrino masses.

As an example, we consider the case of vanishing NSI. From Eqs. (A1)-(A3), one can directly write down

$$c_0 = -\frac{1}{(2E)^3} A \Delta_{21} \Delta_{31} |V_{e1}|^2 , \quad (\text{A7})$$

$$c_1 = \frac{1}{(2E)^2} \left\{ \Delta_{21} \Delta_{31} + A \left[\Delta_{21} (1 - |V_{e2}|^2) + \Delta_{31} (1 - |V_{e3}|^2) \right] \right\} , \quad (\text{A8})$$

$$c_2 = -\frac{1}{2E} (A + \Delta_{21} + \Delta_{31}) . \quad (\text{A9})$$

Substituting Eqs. (A7)-(A9) into Eqs. (A4)-(A6), the matter corrected eigenvalues given in Refs. [69, 70] can be reproduced straightforwardly. One may also check that $A = 0$ leads to the limit $\tilde{m}_i = m_i$.

APPENDIX B: FORMULAS FOR EFFECTIVE MIXING MATRIX ELEMENTS

In the limit of small parameters, i.e., $\eta \rightarrow 0$ and $V_{e3} \rightarrow 0$, one can use our main result for the exact analytical parameter mappings Eq. (20) to derive zeroth-order series expansion formulas for the modulus squares of the mixing matrix elements V_{e3} , V_{e2} , and $V_{\mu3}$. The results are given by

$$|\tilde{V}_{e3}|^2 = \frac{1}{\tilde{\Delta}_{31}\tilde{\Delta}_{32}} \left\{ \tilde{m}_1^2 \tilde{m}_2^2 - A(1 + \varepsilon_{ee})(\tilde{m}_1^2 + \tilde{m}_2^2) + A^2 [(1 + \varepsilon_{ee})^2 + |\varepsilon_{e\mu}|^2 + |\varepsilon_{e\tau}|^2] \right\} , \quad (\text{B1})$$

$$|\tilde{V}_{e2}|^2 = \frac{1}{\tilde{\Delta}_{21}\tilde{\Delta}_{23}} \left\{ \tilde{m}_1^2 \tilde{m}_3^2 - A(1 + \varepsilon_{ee})(\tilde{m}_1^2 + \tilde{m}_3^2) + A^2 [(1 + \varepsilon_{ee})^2 + |\varepsilon_{e\mu}|^2 + |\varepsilon_{e\tau}|^2] \right\} , \quad (\text{B2})$$

$$\begin{aligned} |\tilde{V}_{\mu3}|^2 = & \frac{1}{\tilde{\Delta}_{31}\tilde{\Delta}_{32}} \left\{ \tilde{m}_1^2 \tilde{m}_2^2 + \Delta_{31} (\Delta_{31} - \tilde{m}_1^2 - \tilde{m}_2^2) |V_{\mu3}|^2 + A^2 (|\varepsilon_{e\mu}|^2 + |\varepsilon_{\mu\mu}|^2 + |\varepsilon_{\mu\tau}|^2) \right. \\ & \left. - A\varepsilon_{\mu\mu} (\tilde{m}_1^2 + \tilde{m}_2^2) + 2A\Delta_{31} [\varepsilon_{\mu\mu}|V_{\mu3}|^2 + \text{Re}(\varepsilon_{e\mu}V_{e3}V_{\mu3}^*) + \text{Re}(\varepsilon_{\mu\tau}V_{\tau3}V_{\mu3}^*)] \right\} , \end{aligned} \quad (\text{B3})$$

which are valid to all orders in the NSI parameters. In addition, for standard matter effects, i.e., without NSI effects, and for any η and V_{e3} , we can derive the corresponding formula to Eq. (20). The result is

$$\begin{aligned} \tilde{V}_{\alpha i} \tilde{V}_{\beta i}^* = & \frac{1}{\tilde{\Delta}_{im}\tilde{\Delta}_{in}} \left[\sum_j \hat{\Delta}_{jm} \hat{\Delta}_{jn} V_{\alpha j} V_{\beta j}^* + A \delta_{\alpha e} \delta_{\beta e} (A - \tilde{m}_n^2 - \tilde{m}_m^2) \right. \\ & \left. + A \sum_j \Delta_{j1} (\delta_{\alpha e} V_{ej} V_{\beta j}^* + \delta_{\beta e} V_{\alpha j} V_{ej}^*) \right] . \end{aligned} \quad (\text{B4})$$

In the specific cases of V_{e3} , V_{e2} , and $V_{\mu3}$, we obtain

$$|\tilde{V}_{e3}|^2 = \frac{1}{\tilde{\Delta}_{31}\tilde{\Delta}_{32}} \left[\sum_j \hat{\Delta}_{j1} \hat{\Delta}_{j2} |V_{ej}|^2 + A (A - \tilde{m}_1^2 - \tilde{m}_2^2) + 2A \sum_{j=2,3} \Delta_{j1} |V_{ej}|^2 \right] , \quad (\text{B5})$$

$$|\tilde{V}_{e2}|^2 = \frac{1}{\tilde{\Delta}_{21}\tilde{\Delta}_{23}} \left[\sum_j \hat{\Delta}_{j1} \hat{\Delta}_{j3} |V_{ej}|^2 + A (A - \tilde{m}_1^2 - \tilde{m}_3^2) + 2A \sum_{j=2,3} \Delta_{j1} |V_{ej}|^2 \right] , \quad (\text{B6})$$

$$|\tilde{V}_{\mu3}|^2 = \frac{1}{\tilde{\Delta}_{31}\tilde{\Delta}_{32}} \sum_j \hat{\Delta}_{j1} \hat{\Delta}_{j2} |V_{\mu j}|^2 , \quad (\text{B7})$$

which are valid to all orders in the small parameters η and V_{e3} .

[1] Y. Fukuda et al. (Super-Kamiokande), Phys. Rev. Lett. **81**, 1562 (1998), hep-ex/9807003.

- [2] S. Fukuda et al. (Super-Kamiokande), Phys. Rev. Lett. **86**, 5651 (2001), hep-ex/0103032.
- [3] J. P. Cravens et al. (Super-Kamiokande), Phys. Rev. **D78**, 032002 (2008), arXiv:0803.4312.
- [4] Q. R. Ahmad et al. (SNO), Phys. Rev. Lett. **87**, 071301 (2001), nucl-ex/0106015.
- [5] S. N. Ahmed et al. (SNO), Phys. Rev. Lett. **92**, 181301 (2004), nucl-ex/0309004.
- [6] B. Aharmim et al. (SNO), Phys. Rev. Lett. **101**, 111301 (2008), arXiv:0806.0989.
- [7] M. Apollonio et al. (CHOOZ), Phys. Lett. **B466**, 415 (1999), hep-ex/9907037.
- [8] K. Eguchi et al. (KamLAND), Phys. Rev. Lett. **90**, 021802 (2003), hep-ex/0212021.
- [9] M. H. Ahn et al. (K2K), Phys. Rev. Lett. **90**, 041801 (2003), hep-ex/0212007.
- [10] D. G. Michael et al. (MINOS), Phys. Rev. Lett. **97**, 191801 (2006), hep-ex/0607088.
- [11] B. Pontecorvo, Sov. Phys. JETP **6**, 429 (1957).
- [12] Z. Maki, M. Nakagawa, and S. Sakata, Prog. Theor. Phys. **28**, 870 (1962).
- [13] B. Pontecorvo, Sov. Phys. JETP **26**, 984 (1968).
- [14] V. N. Gribov and B. Pontecorvo, Phys. Lett. **B28**, 493 (1969).
- [15] L. Wolfenstein, Phys. Rev. **D17**, 2369 (1978).
- [16] S. P. Mikheyev and A. Y. Smirnov, Sov. J. Nucl. Phys. **42**, 913 (1985).
- [17] M. C. Gonzalez-Garcia, Y. Grossman, A. Gusso, and Y. Nir, Phys. Rev. **D64**, 096006 (2001), hep-ph/0105159.
- [18] A. M. Gago, M. M. Guzzo, H. Nunokawa, W. J. C. Teves, and R. Zukanovich-Funchal, Phys. Rev. **D64**, 073003 (2001), hep-ph/0105196.
- [19] P. Huber and J. W. F. Valle, Phys. Lett. **B523**, 151 (2001), hep-ph/0108193.
- [20] T. Ota, J. Sato, and N.-a. Yamashita, Phys. Rev. **D65**, 093015 (2002), hep-ph/0112329.
- [21] P. Huber, T. Schwetz, and J. W. F. Valle, Phys. Rev. **D66**, 013006 (2002), hep-ph/0202048.
- [22] M. Campanelli and A. Romanino, Phys. Rev. **D66**, 113001 (2002), hep-ph/0207350.
- [23] M. Blennow and T. Ohlsson, Phys. Lett. **B609**, 330 (2005), hep-ph/0409061.
- [24] M. Blennow, T. Ohlsson, and W. Winter, Eur. Phys. J. **C49**, 1023 (2007), hep-ph/0508175.
- [25] M. Honda, N. Okamura, and T. Takeuchi (2006), hep-ph/0603268.
- [26] N. Kitazawa, H. Sugiyama, and O. Yasuda (2006), hep-ph/0606013.
- [27] R. Adhikari, S. K. Agarwalla, and A. Raychaudhuri, Phys. Lett. **B642**, 111 (2006), hep-ph/0608034.
- [28] M. Blennow, T. Ohlsson, and J. Skrotzki, Phys. Lett. **B660**, 522 (2008), hep-ph/0702059.
- [29] J. Kopp, M. Lindner, and T. Ota, Phys. Rev. **D76**, 013001 (2007), hep-ph/0702269.

- [30] N. C. Ribeiro, H. Minakata, H. Nunokawa, S. Uchinami, and R. Zukanovich-Funchal, JHEP **12**, 002 (2007), arXiv:0709.1980.
- [31] J. Kopp, M. Lindner, T. Ota, and J. Sato, Phys. Rev. **D77**, 013007 (2008), arXiv:0708.0152.
- [32] J. Kopp, T. Ota, and W. Winter, Phys. Rev. **D78**, 053007 (2008), arXiv:0804.2261.
- [33] M. Blennow, D. Meloni, T. Ohlsson, F. Terranova, and M. Westerberg, Eur. Phys. J. **C56**, 529 (2008), arXiv:0804.2744.
- [34] W. Winter, Phys. Lett. **B671**, 77 (2009), arXiv:0808.3583.
- [35] G. Altarelli and D. Meloni, Nucl. Phys. **B809**, 158 (2008), arXiv:0809.1041.
- [36] T. Kikuchi, H. Minakata, and S. Uchinami, JHEP **03**, 114 (2009), arXiv:0809.3312.
- [37] T. Ohlsson and H. Zhang, Phys. Lett. **B671**, 99 (2009), arXiv:0809.4835.
- [38] A. Bueno, M. Campanelli, M. Laveder, J. Rico, and A. Rubbia, JHEP **06**, 032 (2001), hep-ph/0010308.
- [39] M. Malinský, T. Ohlsson, and H. Zhang, Phys. Rev. **D** (to be published), arXiv:0811.3346.
- [40] M. Blennow and T. Ohlsson, Phys. Rev. **D78**, 093002 (2008), arXiv:0805.2301.
- [41] Y. Farzan and A. Y. Smirnov, Phys. Rev. **D65**, 113001 (2002), hep-ph/0201105.
- [42] Z. Berezhiani and A. Rossi, Phys. Lett. **B535**, 207 (2002), hep-ph/0111137.
- [43] S. Davidson, C. Peña Garay, N. Rius, and A. Santamaria, JHEP **03**, 011 (2003), hep-ph/0302093.
- [44] J. Barranco, O. G. Miranda, C. A. Moura, and J. W. F. Valle, Phys. Rev. **D73**, 113001 (2006), hep-ph/0512195.
- [45] J. Barranco, O. G. Miranda, C. A. Moura, and J. W. F. Valle, Phys. Rev. **D77**, 093014 (2008), arXiv:0711.0698.
- [46] Y. Grossman, H. E. Haber, and Y. Nir, Phys. Lett. **B357**, 630 (1995), hep-ph/9507213.
- [47] S. Antusch, C. Biggio, E. Fernández-Martínez, M. B. Gavela, and J. Lopez-Pavon, JHEP **10**, 084 (2006), hep-ph/0607020.
- [48] H. Zhang and Z. Z. Xing, Eur. Phys. J. **C41**, 143 (2005), hep-ph/0411183.
- [49] Z. Z. Xing and H. Zhang, Phys. Lett. **B618**, 131 (2005), hep-ph/0503118.
- [50] H. Zhang, Mod. Phys. Lett. **A22**, 1341 (2007), hep-ph/0606040.
- [51] J. Kopp, Int. J. Mod. Phys. **C19**, 523 (2008), physics/0610206.
- [52] K. Kimura, A. Takamura, and H. Yokomakura, Phys. Lett. **B537**, 86 (2002), hep-ph/0203099.
- [53] K. Kimura, A. Takamura, and H. Yokomakura, Phys. Rev. **D66**, 073005 (2002), hep-

ph/0205295.

- [54] O. Yasuda (2007), arXiv:0704.1531.
- [55] C. Jarlskog, Phys. Rev. Lett. **55**, 1039 (1985).
- [56] E. K. Akhmedov, R. Johansson, M. Lindner, T. Ohlsson, and T. Schwetz, JHEP **04**, 078 (2004), hep-ph/0402175.
- [57] T. Schwetz, M. Tórtola, and J. W. F. Valle, New J. Phys. **10**, 113011 (2008), arXiv:0808.2016.
- [58] M. Freund, Phys. Rev. **D64**, 053003 (2001), hep-ph/0103300.
- [59] P. F. Harrison, D. H. Perkins, and W. G. Scott, Phys. Lett. **B530**, 167 (2002), hep-ph/0202074.
- [60] Z. Z. Xing, Phys. Lett. **B533**, 85 (2002), hep-ph/0204049.
- [61] P. Huber, T. Schwetz, and J. W. F. Valle, Phys. Rev. Lett. **88**, 101804 (2002), hep-ph/0111224.
- [62] A. Cervera et al., Nucl. Phys. **B579**, 17 (2000), hep-ph/0002108.
- [63] A. Donini, D. Meloni, and P. Migliozzi, Nucl. Phys. **B646**, 321 (2002), hep-ph/0206034.
- [64] D. Autiero et al., Eur. Phys. J. **C33**, 243 (2004), hep-ph/0305185.
- [65] A. Donini, K.-i. Fuki, J. López-Pavón, D. Meloni, and O. Yasuda (2008), arXiv:0812.3703.
- [66] M. Guler et al. (OPERA) (2000), cERN-SPSC-2000-028.
- [67] T. Ohlsson and H. Snellman, J. Math. Phys. **41**, 2768 (2000), hep-ph/9910546.
- [68] T. Ohlsson and H. Snellman, Phys. Lett. **B474**, 153 (2000), hep-ph/9912295.
- [69] V. D. Barger, K. Whisnant, S. Pakvasa, and R. J. N. Phillips, Phys. Rev. **D22**, 2718 (1980).
- [70] H. W. Zaglauer and K. H. Schwarzer, Z. Phys. **C40**, 273 (1988).